Title	Dynamic increment for shear force due to heavy vehicles crossing a highway bridge
Authors(s)	González, Arturo; Cantero, Daniel; O'Brien, Eugene J.
Publication date	2011-12
Publication information	Computers and Structures, 89 (23-24): 2261-2272
Publisher	Elsevier
Link to online version	http://dx.doi.org/10.1016/j.compstruc.2011.08.009
Item record/more information	http://hdl.handle.net/10197/3426
Publisher's statement	þÿ T h i s i s t h e a u t h o r s v e r s i o n o f a w o r k t h a t w a s a c c e p t e d f o Changes resulting from the publishing process, such as peer review, editing, corrections, structural formatting, and other quality control mechanisms may not be reflected in this document. Changes may have been made to this work since it was submitted for publication. A definitive version was subsequently published inComputers and Structures, 89 (23-24): 2261-2272 DOI: 10.1016/j.compstruc.2011.08.009
Publisher's version (DOI)	10.1016/j.compstruc.2011.08.009

Title

Dynamic increment for shear force due to heavy vehicles crossing a highway bridge

Authors

A. González[1,*], D. Cantero[1,2] and E.J. OBrien[1,3]

Affiliations

[1]School of Architecture, Landscape and Civil Engineering, University College Dublin, Dublin, Ireland

[*]corresponding author, email: arturo.gonzalez@ucd.ie, telephone: +353-1-7163219, fax: +353-1-7163297

[2]email: canterolauer@gmail.com, telephone: +353-1-7163233, fax: +353-1-7163297

[3]email: eugene.obrien@ucd.ie, telephone: +353-1-7163224, fax: +353-1-7163297

Abstract

Most of the current research on dynamic amplification factors caused by traffic flow on a bridge has focused on bending moment effects. Although bending stresses often govern the requirements of the bridge section, sufficient shear capacity must be provided too. Shear stresses near the support are strongly influenced by damaged expansion joints and/or differential settlements between the bridge deck and the approach road. The latter is taken into account in this theoretical investigation to evaluate the dynamics associated with the shear load effect caused by heavy trucks and how it relates to the length of the bridge span.

Keywords

vehicle; bridge; dynamics; shear; expansion joint.

1 Introduction

Bridges are more likely to fail in bending than shear after significant plastic deformation has developed under excessive dynamic traffic load [1], and the most unfavourable scenario for bridge elements is the impact-like excitation of passing vehicles by singular irregularities. Brittle failure mechanisms such as shear failures are not so frequent, but if an accurate assessment is needed or if there are signs of cracking initiating close to the support, the applied shear force and structural shear strength will require immediate attention. Particular caution must be used when dealing with old bridge girders that may be lightly reinforced for shear following design specifications at the time [2].

The roughness of the road profile is a major factor influencing the response of the bridge to a passing vehicle [3] as well as specific locations of bumps [4]. Increments with respect to the static response of 10% for smooth approach and deck conditions, 20% for rough road profile with bumps and 30% for extreme conditions of high speed, short span (< 12m) and poor road profile are typical dynamic allowances used in the assessment of existing highway bridges [5]. Kim et al. [6] shows the best way of reducing dynamics effects due to a bump is by removing it. However, there are certain types of discontinuities that frequently appear on the road profile prior to a bridge, i.e., at the expansion joint. Either because expansion joints are frequently the weak point of bridges [7] and are easily damaged or because differential settlements occur between the bridge and the abutment, it is not rare to have a significant discontinuity at this location. Any step on the road surface influences the vehicle dynamics and subsequently the

bridge response. In [8-10], it can be seen how a single bump or ramp can be positioned in some critical location where the bridge response due to a moving vehicle will be of major significance. In [11], combinations of bump characteristic (i.e., height and length) and vehicle speed can result in very high dynamic effects. Despite the damping of the vehicle suspension that rapidly dissipates the vertical movements of the vehicle due to a bump, high impact forces occur near the start of the bridge [12], which are likely to produce high shear loading effects.

Dynamic shear forces due to moving loads can be found in analytical studies [13-17]. However, only a reduced number of authors address the effects of dynamic shear forces in vehicle-bridge interaction (VBI) problems. Huang et al. [18] investigates the response of a horizontally curved bridge due to the crossing of a sprung vehicle model with fixed mechanical properties that represents the HL-93 truck as described in AASHTO specifications, and states that the shear forces are influenced more by higher modes of vibration of the bridge when compared to mid-span bending moment. In [19], this work is continued taking into account the road roughness and presenting simplified expressions for shear impact factors, being in general smaller than for bending moment. A similar conclusion was reached for high speed trains travelling at resonant speeds on Euler-Bernoulli beams [20].

Bridge codes quantify the dynamic increment due to VBI through the application of a factor to the design static load effect. In AASHTO [21], a unique dynamic increment of 30% is defined for any span shorter than 40m, and this dynamic increment decreases as span length increases for spans longer than 40m. The live-load model in AASHTO

LRFD [22] is made of a design truck and a design lane load, and a dynamic load allowance of 1.15 is specified for fatigue and fracture, and 1.33 for all other limit states to be applied only to the design truck. However, different values are specified for individual components of the bridge such as deck joints.

The Eurocode [23] establishes different traffic load models with built-in dynamic amplification factors (DAFs) defined as the ratio of total to static load effect. The latter are based on dynamic factors obtained from numerical simulations and combined statistically with the static results to obtain the characteristic values for each load model [24]. For one-lane bridges, Eurocode uses smaller DAF values for shear than for bending moment. Up to 5m spans, there is a constant value of DAF for moment and shear given by 1.7 and 1.4 respectively. Then, DAF for moment decreases linearly from 1.7 (5m span) to 1.4 (15m span), and it remains constant at 1.4 for spans longer than 15m. DAF for shear decreases linearly from 1.4 (5m span) to 1.2 (25m span), and a 1.2 value is employed for spans longer than 25m. For two-lane bridges up to 50 m span, built-in DAF values are based on a linear variation with span length L, as given by Equation (1), and they are the same for shear and bending moment.

$$DAF = 1.3 - \frac{0.4}{100}L \qquad \text{for } L \leq 50m \tag{1}$$

Furthermore, an additional DAF is recommended near expansion joints, $\Delta\varphi$ (Equation (2)) and applied to all loads in the fatigue limit state.

$$\Delta\varphi = 1.3\left(1 - \frac{D}{26}\right) \qquad \text{for } \Delta\varphi \geq 1 \tag{2}$$

where *D* is the distance in meters of the cross-section under consideration from the expansion joint.

Brüwler and Herwig [1] calculate the ultimate limit state DAF values according to two different failure modes, significant- and small-deformation capacity. For bending moments and displacements, significant deformations occur, yielding to plastic response of the structure and increasing the dissipation capacity of the element, inferring that no amplification factor is needed (DAF = 1). However, for failure modes with small deformation capacity, such as due to shear forces, no sufficient dissipation capacity is available and DAF values are suggested according to span length (Figure 1).

Figure 1: Dynamic amplification factors for failure modes with small deformation [1]

Shear is going to be influenced by torsion and transverse modes of vibration, which will become more important in skewed and curved bridges. For I-girder curved bridges with less than two continuous spans, span lengths between 15.24 and 60.96m, radii between 60.96 and 304.8m and 6 or less girders, AASHTO [5] proposes DAF values of 1.3 for shear, 1.25 for moment in longitudinal girders, 1.40 for torsion in longitudinal girders and 1.20 for moments in slab. In the case of curved box girders, those AASHTO recommendations [5] vary with span length and radius, and DAF values are between 1.173 and 1.215 for shear, between 1.240 and 1.320 for primary bending moment, and between 1.260 and 1.308 for torsion. Huang [19] uses 3D VBI models and field results to show that the DAFs for torsion in curved box girder bridges increase more rapidly

with vehicle speed than moment, shear, or deflection. However, the smaller the radius of curvature, the smaller the maximum allowable speed, and hence, moment, shear, and deflection impact factors for curved bridges are normally smaller than those corresponding to straight bridges. He finds AASHTO recommendations for DAF of shear in curved box girder bridges to be too conservative and he proposes 1.16 and 1.20 for vertical shear and bending moment respectively. It must be noted that DAF values for critical loading cases of continuous structures are typically smaller than for single span structures.

The general expressions for DAF shear at the support in Equations (1) and (2) do not allow for different vehicle types or conditions of the expansion joint (larger bumps will cause higher impact forces and dynamic amplification of shear). The influence of the expansion joint and the profile on DAF is strongly related to the bridge span (In a critical traffic loading event, long span bridges allow for many axles simultaneously on the bridge, and while some of these axles may be highly excited by a bump, the vibrations of the remaining axles will have damped out considerably, leading to smaller DAFs than short span bridges). It is the aim of this paper to evaluate the DAF for shear at the support as function of the bridge length for single and multiple vehicle events travelling over smooth and rough road profiles with three conditions of the joint at the support: healthy, a 2cm bump and a 4cm bump. Furthermore, Weigh-In-Motion (WIM) records have shown that extremely heavy vehicles, such as cranes, are becoming more and more frequent in normal traffic [25]. As a result, these extreme vehicles appear to govern the critical traffic load effects of many simply supported short to medium span

bridge sites, and their effect on the dynamic component of the bridge response is subject of investigation here.

This article is a substantially extended and revised version of a paper presented at Civil-Comp [26]. In the latter, the dynamic effects of large cranes on the shear load effect in short to medium span bridges were compared to typical 5-axle articulated trucks using planar VBI models. In the current paper, the number of spans under investigation is increased, the analysis of shear is performed for each support independently, the dynamic increment of bending moment at mid-span associated to each shear result is included for comparison purposes, and shorter spans where the differences between shear and bending moment are greater are analysed in more detail. Shear and bending load effects are obtained for a wide range of VBI parameters varied using Monte Carlo simulation. The condition of the expansion joint is modelled according to inspection surveys and the properties of the vehicles are randomly sampled from distributions that adequately represent actual highway traffic.

.

2 Simulation Model

From a static point of view, a moving load will cause highest shear and bending moment at the supports and the mid-pan section respectively of a simply supported beam. The dynamic amplification of shear and bending stresses are calculated at these locations using the combined method outlined by Frỳba [13]. The coupled vehicle and bridge system is solved using the Wilson-θ integration scheme [27]. A description of the vehicle, bridge and road profile models used in the simulations follows.

2.1 Vehicle

The vehicle models are represented as lumped masses joined to the road or bridge surface by spring-dashpot systems that simulate the suspension and tyre responses. Figures 2a and 2b show sketches of the 5-axle truck and crane models respectively. The main difference between both models is the presence of a hinge in the articulated truck allowing it to be more flexible than the crane. In addition, the number of axles, spacing and loads are different for both models. The vehicle responses are obtained using a planar model following Cantero et al. [28], that present the equations of motion for a general articulated road vehicle, with variable numbers of wheels for the tractor and semitrailer. Similar vehicle models have been widely used in the literature representing VBI with a reasonable degree of accuracy [29-31].

Figure 2: Vehicle model sketch: a) 5-axle truck; b) Crane (all dimensions in m)

The parameters of the 5-axle truck have been chosen to represent a typical European heavy truck [32, 33]. For the 9-axle crane, body masses, axle spacings and loads are based on crane manufacturer specifications and WIM data, while other parameters such as suspension and tire properties have been taken from the literature for a similar vehicle by Li [34] and Lehtonen et al. [35] that provide results from extensive experimental tests. The dynamic properties and statistical variability used in the Monte Carlo simulations are summarised in Table 1 for both vehicles.

Table 1: Truck and crane mechanical parameters

2.2 Beam

In a real 3-dimensional situation, shear will also depend on twisting moments and it is going to be more important at the edges and near discrete support locations than for other transverse locations. Nevertheless, a beam model can provide a useful insight into the mechanisms triggering the dynamics of shear in straight non-skewed bridges with predominant longitudinal bending. In this paper, the bridge is modelled as a simply supported Euler-Bernoulli beam of length L with an overhang of L_e as shown in Figure 3, and constant cross section and mass per unit length. Although some studies [15, 39] recommend the use of Timoshenko beams to take into account shear deformation, shear deformation is generally not very significant in typical short- and medium-span bridges [40] and in this case, Esmailzadeh and Ghorashi [41] show that for simply supported beams there is good agreement in responses for both formulations. Some researchers point out that shear analysis requires a large number of modes of vibration compared to displacement or moment to converge to the static response at the discontinuities [42-44]. However, the approach presented by Frỳba [13] is used in this paper, where the stresses are calculated using the combined method, that splits the calculation into a quasi-static component and an inertial component, which converges to the solution rapidly. The quasi-static component refers to the contribution of the vehicle forces to a given load effect. The latter is given by the sum for all axles on the bridge of the products of each axle force (static + dynamic) by the corresponding ordinate of the influence line for the load effect being sought. The inertial component here refers to the contribution to load effect that comes from the bridge's mass in motion. Only 6 modes of vibration are included in the VBI model presenting no significant difference when

more modes were considered. If the vehicle model consisted of moving constant loads (i.e., if vehicle dynamics were ignored), the quasi-static and inertial components of the response will be equal to the static and dynamic components respectively.

Figure 3: Bridge model

Table 2 summarises properties for the bridge spans tested in the simulations. These properties are based on bridge cross-sections made of T beams, Y beams or Super-Y beams depending on the bridge span [45]. Bridge responses are simulated for a total of 53 spans (values are interpolated for those spans not included in Table 2). Young's Modulus of $3.5 \times 10^{10} \text{N/m}^2$ and 3% viscous damping factor (ξ, as defined by the logarithmic decrement of damping in Equation (3)) are adopted for all bridge spans.

$$\frac{\xi}{\sqrt{1-\xi^2}} = \ln \frac{u_n - u_1}{2\pi N} \tag{3}$$

where N is the number of oscillations in free vibration between two non-consecutive peak displacements (u_n and u_1).

Table 2: General characteristics of the bridge models

These models assume that the influence of the foundation, soil and bearing compressibility on the bridge response is negligible and that the superstructure can be analyzed in isolation from the substructure. In the case of neoprene pad supports,

Memory et al. [46] have found that their stiffness hardly affect the fundamental frequency of a beam. Therefore, the results here only refer to good foundations and well maintained stiff bearings.

2.3 Road Profile and Damaged Expansion Joint

The profiles are generated as a random stochastic process described by a power spectral density (*PSD*) function as specified in the ISO recommendations [47] for each spatial frequency Ω_i and road class. Road classes can be varied from 'A' (very good) to 'E' (very poor), although well maintained highway pavements are assumed in this paper and only class 'A' profiles are employed. The road surface irregularities, $r(x)$, are generated as a function of distance x from the left end of the profile, using Equation (4).

$$r(x) = \sum_{i=1}^{N} \sqrt{2PSD_i \Delta\Omega} \cos(2\pi\Omega_i + \theta_i) \qquad (4)$$

where N is the total number of waves used to construct the road surface, $\Delta\Omega$ is the frequency interval ($\Delta\Omega = (\Omega_{max} - \Omega_{min})/N$, where Ω_{min} and Ω_{max} are 0.01 and 4 cycles/m respectively), and θ_i is the phase angle that corresponds to the spatial frequency Ω_i, which is defined by Equation (5).

$$\Omega_i = \Omega_{min} + (i - 0.5)\Delta\Omega \qquad i = 1, 2, 3...N \qquad (5)$$

The *PSD* is directly proportional to the spatial geometric mean, which can adopt a range of values that depends on the selected road class. N is chosen to be 400 frequency

components in all simulations. The randomness of the profile is derived from the selected spatial geometric mean value and phases for each spatial wave/frequency. These parameters are sampled based on an assumed uniform distribution for both spatial geometric mean [from $4x10^{-6}$ to $8x10^{-6}m^3$/cycle for a class 'A' profile] and phase [from 0 to 2π] variables. A moving average filter (24cm long patch) is applied to the profile to smooth it and simulate the effect of the tire footprint. An approach length of 100m is also employed to excite the vehicle prior to the bridge. In the case of meeting events, the approach length for one of the vehicles might be greater than 100m depending on its speed and the meeting point of both vehicles on the bridge.

The shape used to model the bump is shown in Figure 4a. For fixed width and depth dimensions, alterations of the bump shape do not appear to cause significant variations on the bridge response. In this paper, 2cm deep bumps are used to represent average damaged expansion joints, and 4cm is the maximum depth considered. These values are based on expansion joints road network surveys from Japan [48,49] and Portugal [7]. The bumps are located at 0.5m from bridge support to account for the usual beam overhang (L_e in Figure 3). Figure 4b gives the profile resulting from combining a class A road profile and a 2cm deep bump.

Figure 4: a) Damaged expansion joint (all dimensions in cm, *h*: bump height); b) Example of road profile with 2cm deep bump

3 Single Vehicle Events

The DAFs for shear forces at the supports and bending moment at mid-span are analysed here for single vehicle events. First, a preliminary analysis using a constant load is carried out to give an order of magnitude of the DAF values when the surface is assumed to be smooth and vehicle dynamics are ignored. Then, the additional dynamics due to the influence of the road profile and bumps on vehicle sprung models and bridge responses are discussed.

3.1 Vehicle Model based on a Moving Single Constant Force

Using the closed form solution for a single constant load over a simply supported Euler-Bernoulli beam [13,14], it can be shown that the DAFs for shear at supports are in some situations larger than for bending moment at mid-span. This phenomenon is illustrated in Figure 5, where frequency ratio (FR) is defined by Equation (6):

$$\mathrm{FR} = \frac{c}{2 f_1 L} \tag{6}$$

where c is the speed of the vehicle in m/s, f_1 the first natural frequency of the bridge in Hz and L the span length in m. Dynamic peaks develop at different values of FR for shear and moment as a result of a critical combination of speed of the moving load, bridge length and frequency.

Figure 5: Dynamic amplification factors versus frequency ratio due to a moving constant load; shear at 1st support (solid line), bending moment (dotted line), shear at 2nd support (dashed line)

Therefore, shear DAF values are distinctively different according to the support under consideration. The static shear load effect is the same at both end supports, but when the load reaches the 1st support there has been little or no time for the bridge to be dynamically altered. As result, dynamic factors for shear forces at first support are small, they show little sensitivity to changes in FR, and they tend to be slightly under the unit value. On the other hand, when the load leaves the beam, the system has had time to develop a distribution of bridge inertial forces that may result into a large total shear force at the 2nd support.

From Figure 5, it is possible to distinguish a number of critical values of FR leading to peaks in the oscillating pattern of dynamic increments of shear and bending moment. The values of FR leading to the highest values of bending and shear are 0.37 (DAF = 1.40) and 0.92 (DAF = 2.09) respectively. For a bridge span of 12m (7.143Hz as 1st natural frequency), values of FR of 0.37x2f_1L and 0.92x2f_1L correspond to speeds of 228km/h and 568km/h respectively. The horizontal axis of Figure 5 can be converted to speed c, scaling it by $2Lf_1$ for a beam of length L and frequency f_1 (Equation (6)). The DAF-speed pattern within a typical highway speed range (50 to 120 km/h) corresponding to a 12m bridge with f_1 = 7.143Hz is illustrated in Figures 6a and 6b for mid-span moment and shear at the 2nd support respectively. There are a number of critical speeds leading to peak dynamic excitation, i.e., 56km/h (DAF = 1.05) and 90km/h (DAF = 1.10) in Figure 6a for moment, and 82km/h (DAF = 1.04) and 111km/h (DAF = 1.067) amongst others in Figure 6b for shear. These values can also be obtained from the Figure 5, valid for any beam length. For example, the peak at 82km/h

corresponds to peak at a FR of 0.133. Therefore, Figure 6 is identical to Figure 5 if only the portion of the latter with FR values between 0.081 (50km/h) and 0.194 (120km/h) was represented.

Figure 6: Dynamic amplification factors versus speed for a constant load moving on a 12m bridge; a) bending moment, b) shear at 2nd support

For the speed of 56km/h, the static and dynamic components of the total moment at mid-span of a 12m bridge are represented in Figure 7. Given that the mid-span location is considered, even modes have a null effect and odd modes higher than the first mode have a negligible influence on the dynamic component. In this figure, the static component reaches a peak at the same time (0.386s) as the oscillating pattern of the inertial component due to the 1st mode of vibration of the bridge, this matching effect being the cause of high dynamic excitation at this speed. The dynamic component is defined by a series of waves with frequency equal to that of the bridge and decaying amplitude with time. A similar pattern can be found for higher critical speeds, except that there will be a smaller number of waves and their amplitude will be larger, which explains the occurrence of higher dynamic amplifications. For example, Figure 6a shows how a DAF value of 1.05 can be obtained with a critical speed of 56km/h, while 1.10 and 1.40 can be obtained for critical speeds of 90km/h and 228km/h respectively.

Figure 7: Mid-span bending moment response of a 12m bridge due to a single constant load travelling at speed of 56km/h: Total bending moment (solid line), static component (dashed line), dynamic contribution of inertial forces of 1st mode (dotted line)

Figure 8 shows the contribution to shear by component for a critical speed of 82km/h. The ratio of the contribution of the dynamic component to the total is similar to that found in Figure 7 for moment (DAF values of 1.05 and 1.04 in Figures 7 and 8 respectively). Again, the dynamic peak is the result of the time-varying inertial component reaching a maximum when the load is located at the section under investigation (i.e., above the 2nd support, 0.527s after entering the bridge).

Figure 8: Shear response at 2nd support of a 12m bridge due to a single constant load travelling at a speed of 82km/h; Total shear force (solid line), static component (dashed line), dynamic contribution of inertial forces of 1st mode (dotted line)

The contribution of the inertial bridge forces to total shear of Figure 8 is separated by mode of vibration in Figure 9. As for bending moment, the first mode clearly governs the dynamic response, and it has a time-varying sinusoidal shape of decaying amplitude.

Figure 9: Dynamic contribution of inertial forces of the bridge to the shear at 2nd support of a 12m bridge due to a single constant load travelling at a speed of 82km/h; 1st mode (solid line), 2nd mode (dashed line), 3rd mode (dotted line)

González et al. [50] show that a vehicle model consisting of constant forces simulating the static axle weights and spaced as in the real vehicle may be unable to quantify the true dynamic amplification as a result of the road profile and vehicle dynamics, but it can be used to provide reasonable estimates of critical speeds for a given vehicle

configuration on bridges with good road profiles. Therefore, the DAF-speed pattern associated with a typical 5-axle vehicle model based on constant forces with mean values of axle weights and spacings as defined Table 1 is illustrated in Figure 10. Compared to the response of a single constant force model (Figures 6a and 6b), the presence of several vertical forces cause considerable variations of load effects with speed, particularly in the case of shear at 1st support which remained almost constant in Figure 5. For a given bridge, DAFs can be high or low due to the constructive or destructive interference between the contributions of each axle, that depend on speed, magnitudes and spacings of the axle loads. Although it is unlikely that all axles will contribute with a dynamic peak to the total load effect at the same time, the action of some axles may be amplified by an initial vibratory condition of the bridge imposed by preceding axles. In this case, maximum DAF values of 1.029 for shear at the 1st support (at a speed of 70km/h), 1.073 for moment (at 77km/h) and 1.060 for shear at the 2nd support (at 109.5km/h) are evident in Figure 10 within a typical highway speed range, compared to maximum DAFs of 1.10 (moment) and 1.067 (shear at 2nd support) due to a single point load.

Figure 10: Dynamic amplification factors versus speed for a 5-axle truck model consisting of constant loads on a 12 m bridge; shear at 1st support (solid line), bending moment (dotted line), shear at 2nd support (dashed line)

3.2 Sprung Vehicle Models

The models described in Section 2 are employed to analyse the influence of road roughness and expansion joints on the dynamic amplification of the shear and moment

load effects. For instance, the time histories for bending moment at mid-span and shear at 1st support are presented in Figure 11 for the case of a 5-axle truck (with air suspension) travelling at 60km/h over a 12m beam with a smooth profile and a 2cm deep bump (Figure 4) at the bridge entrance (Figure 3). Static component, inertial component due to the first six modes of vibration and total load effect are shown in the figure. Sudden jumps in the shear time history can be observed in Figure 11b every time an axle enters the bridge, and for this particular case the maximum shearing load effect occurs when the last axle of the 5-axle truck enters the bridge. In general, maximum shear forces occur when the entire vehicle is on the bridge and very close to the support, whereas the maximum bending moment usually takes place when the centre of gravity of the vehicle vertical loads is at mid-span. The load distribution between axles determines which truck location is most critical in the case of short span bridges where the vehicle wheelbase may exceed the span length. In Figure 11a, the maximum moment is 632.3kNm, and it occurs when the 1st axle is at 14.14m from the 1st support, where the inertial component due to the bridge is 51.3kNm, the static component is 585.9kNm and the quasi-static component (= total response – inertial component) is 581kNm (i.e., only 4.9kNm or 0.83% higher than the static component).This indicates that most of the dynamic component (= total response – static component) is due to the inertial component of the bridge. On the other hand, the maximum shear is 269.6kN and it occurs when the 1st axle is at 10.36m from the 1st support, where the inertial component is 1.95kN, the static component is 249.8kN and the quasi-static component is 267.65kN (i.e., 17.85kN or 7.14% higher than the static component). In these figures, DAF for shear is 1.072 (269.6kN / 251.5kN) whereas DAF for bending is 1.079 (632.3kNm / 585.9kNm), and they are larger than those obtained in Section 3.1 due to

the influence of the bump (In Figure 10, DAFs at 60 km/h are 0.981 and 1.05 for shear at 1st support and bending moment respectively). While the source of the dynamic increment of bending moment in Figure 11a is mostly attributed to the inertial forces of the bridge, the dynamic increment of shear in Figure 11b is mainly caused by the dynamic forces of the vehicle.

Figure 11: Total (solid line), static (dashed line) and inertial (dotted line) components for load effects due to a 5-axle truck travelling at 60km/h on a 12m span with a 2cm bump; a) Mid-span bending moment; b) Shear force at 1st support

Dynamic Increment (DI) is defined in Equation (7) to evaluate the influence of a damaged expansion joint. DAF values are compared by means of DI for similar situations that only differ in the presence or absence of a bump.

$$\mathrm{DI} = \mathrm{DAF}_{\mathrm{Bump}} - \mathrm{DAF}_{\mathrm{No\ bump}} \qquad (7)$$

The beam stresses are going to be strongly influenced by the condition of the road profile and expansion joint as well as by the mechanical characteristics of the vehicles. For this reason the influence of the bump is studied first for a particular vehicle and a range of speeds (50 – 120km/h), whereas a Monte Carlo simulation is performed later to account for the huge variability in mechanical properties.

Figure 12a presents DAF values for the three load effects under consideration due to a 5-axle truck with the mean values specified in Table 1 over a 12m span and a perfectly

smooth profile. Maximum DAFs of 1.03 (at 70km/h), 1.07 (at 77km/h) and 1.06 (at 110kmh) are obtained for shear at 1st support, moment and shear at 2nd support respectively. As expected, Figure 12a closely resembles Figure 10, given the relatively low vehicle dynamics, only induced by bridge deflection. Figure 12b presents DI due to a 2cm bump at the 1st support when the bridge is traversed by the same vehicle. The axle of the vehicle that enters the bridge suffers a big disruption by the presence of the bump, and it imposes a significant impact force on the bridge that produces high shear forces at the 1st support. However, these oscillations vanish fast and they do not affect the stresses at mid-span or at 2nd support to the same extent. As a result, mid-span bending moment and shear at 2nd support present similar values to those without bump (DI < 0.04). However, the shear force at 1st support always leads to positive and larger DI values than the other two load effects due to the proximity of the bump. These DI values at the 1st support become more important for lower speeds (i.e., 0.15 for 50km/h compared to 0.02 for 120km/h).

Figure 12: Shear 1st support (solid line), Shear 2nd support (dashed line) and bending moment mid-span (dotted line) due to a 5-axle truck on a 12m span with a smooth profile; a) Dynamic amplification factors without a bump; b) Dynamic increments due to a 2cm bump

Up to this point, the analysis has been based on a smooth profile to analyse the influence of a bump on the results in isolation from the road roughness. In all remaining simulations, a class 'A' profile is assumed for the bridge surface and its approach. A 5-axle truck with mean values of mechanical properties (Table 1) is driven over four

hundred 12m beams, each with a different class 'A' profile (randomly generated according to Section 2.3 to cover a range of spatial geometric means and phases). The DAF value is obtained for each random profile and the mean DAF is computed from the 400 profiles and represented in Figure 13a. There are no significant differences between the mean results for a class 'A' profile (Figure 13a) and for a perfectly smooth profile (Figure 12a). Maximum DAFs of 1.03 (at 69km/h), 1.07 (at 77km/h) and 1.06 (at 108km/h) are obtained for shear at 1st support, moment, and shear at 2nd support respectively, which closely resemble those values found in Figure 12a for a smooth profile. The standard deviation of the 400 profiles is represented for a range of speeds in Figure 13b. Standard deviation tends to increase with speed, being higher for bending moment than for shear. The dynamic excitation of the beam is generally more important for higher vehicle speeds, and hence, the scatter introduced by the road randomness also becomes greater. Nevertheless, the magnitude of the dispersion introduced by class 'A' profiles is generally small (maximum standard deviations of 0.030, 0.040 and 0.032 for shear at 1st support, moment and shear at 2nd support respectively) compared to a smooth profile. The analysis is repeated allowing for a 2cm bump at the 1st support that is superposed on each random road profile. The DI values computed from the means of the 400 profiles with and without bump are represented in Figure 13c. The latter is very similar to Figure 12b without a rough profile and it shows that for a 12m bridge, the bump singularity governs the vehicle/bridge response over the roughness for a class 'A' profile.

Figure 13: Shear 1st support (solid line), shear 2nd support (dashed line) and bending moment mid-span (dotted line) due to a 5-axle truck on 12m span with a class 'A' road

profile: a) Dynamic amplification factors (mean value) without a bump; b) Dynamic amplification factors (standard deviation) without a bump; c) Mean dynamic increments due to a 2cm bump

In the figures that follow, the 5-axle truck and crane are studied independently within a Monte Carlo simulation scheme for 53 bridge spans and three bump depths (0, 2 and 4cm) located at the approach, close to the first support. Vehicle parameters are varied within a realistic range of values (Table 1), including speed, suspension and tyre mechanical properties, as well as different profiles (although within the same class 'A') for each event. Figures 14a, 14b and 14c show the mean shear DAF at the 1st support, mean bending moment DAF at mid-span and mean shear DAF at the 2nd support respectively for the 5-axle truck population. Each point in the figures represents the average value for more than 700 events, adding up to more than 114000 simulations. There is a clear influence of bridge length on DAF. DAF typically decreases as the span increases for lengths smaller than 20m or 15m in the case of shear at 1st support or moment respectively. For spans longer than 20m, the mean DAF tends to remain constant for a specified bump depth. A distinctive feature from the results is that the effect of the bump is noticeable on DAF for shear at the 1st support for every span under investigation due to the proximity of the irregularity. However, the influence of bump depth on DAF for bending moment and shear at 2nd support is hardly noticeable for spans greater than 10m.

Figure 14: Mean DAF due to 5-axle truck on class 'A' profile; No damage (•-•-•-•-); 2cm bump depth (x-x-x-x-), 4cm bump depth (*-*-*-*-); a) Shear force at 1st support; b) Bending moment; c) Shear force at 2nd support

Figure 15 shows the standard deviation associated with the mean values calculated in Figure 14. As expected, the standard deviations for a 12m bridge without a bump (0.038, 0.044 and 0.037 for shear at 1st support, moment and shear at 2nd support respectively), where both profile and vehicle properties are randomly varied, appears to be somewhat larger than those found in figure 13b for a range of speeds where each point corresponds to a population of many profiles but only one vehicle. For spans longer than 12m, the standard deviation is approximately 0.05. The presence of a bump becomes important for span lengths shorter than 12m where the standard deviation increases (up to a maximum of 0.141, 0.234 and 0.167 for shear at 1st support, moment and shear at 2nd support respectively with a 4cm bump at the 1st support) as the span length decreases and the bump gets deeper.

Figure 15: Standard deviation of DAF due to 5-axle truck on class 'A' profile; No damage (•-•-•-•-); 2cm bump depth (x-x-x-x-), 4cm bump depth (*-*-*-*-); a) Shear force at 1st support; b) Bending moment; c) Shear force at 2nd support

The same Monte Carlo study is performed for a fleet of cranes, and the results for mean and standard deviation are presented in Figures 16 and 17 respectively. These figures clearly show smaller and less scattered DAF values than those found in Figures 14 and 15 for the 5-axle articulated truck fleet. The small DAF associated with cranes is due to

the large static load effect, high number of wheels, high vehicle rigidity and high moment of inertia compared to 5-axle trucks. Another conclusion that can be extracted from the simulations is the similarity of mean DAF values and standard deviations regardless of the bump depth. The mean DAF for shear at 1st support due to cranes remain below 1.04 for any span and bump depth (below 1.07 for shear at 2nd support), and the standard deviation varies between 0.027 and 0.060 (between 0.036 and 0.072 for shear at 2nd support). Therefore, DAF for moment due to cranes is not as sensitive to bridge length as DAF due to 5-axle trucks. Mean DAF for moment reaches a maximum of 1.153 for a 5m bridge with a 4cm bump (standard deviation of 0.096) and the mean DAF remains below 1.10 for any span longer than 7m (the standard deviation of DAF for moment associated with spans longer than 7m varies between 0.033 and 0.051).

Figure 16: Mean DAF due to fleet of cranes on class 'A' profile; No damage (•-•-•-•-); 2cm bump depth (x-x-x-x-), 4cm bump depth (*-*-*-*-); a) Shear force at 1st support; b) Bending moment; c) Shear force at 2nd support

Figure 17: Standard deviation of DAF due to fleet of cranes on class 'A' profile; No damage (•-•-•-•-); 2cm bump depth (x-x-x-x-), 4cm bump depth (*-*-*-*-); a) Shear force at 1st support; b) Bending moment; c) Shear force at 2nd support

Numerical values for the mean and standard deviation of total shear load effects due to the 5-axle truck and the crane are provided in Table 3 for some spans up to 15m. It can be seen that cranes generate smaller DAFs than the 5-axle trucks, but Table 3 shows that

they lead to considerably higher values of total shear given the magnitude of their axle forces and their closely spaced axle configurations.

Table 3: Mean and standard deviation of shear force at 1st support due to single vehicle events

The analysis of the single traffic events has shown that the differences between DAF for shear and DAF for bending moment are more important for shorter span lengths, and for a given bump depth, the DAF for shear is typically lower than the DAF for bending moment. Nevertheless, the design load effect of a two-lane bridge usually corresponds to multiple vehicle configurations, which are investigated in the following section.

4 Meeting Events

In the case of short span two-lane bridges (< 20m), the critical traffic loading event consists of two heavy trucks meeting on the bridge [51]. Meeting events involving more than two vehicles are relevant for longer spans, but for short spans, long vehicles' wheelbase is as long as the bridge span, making it difficult to locate more than one vehicle per lane. Two types of meeting events have been defined to compare different traffic scenarios. Type I is defined as two 5-axle trucks meeting on the bridge and type II as a 5-axle truck meeting a crane, as sketched in Figure 18.

Figure 18: Scenarios of vehicle meeting events; a) Type I; b) Type II

The influence of the road profile is investigated using a Monte Carlo simulation consisting of more than 350000 events made of 2 vehicles meeting on the bridge. For each event, profiles, vehicle speeds and mechanical properties and meeting locations are randomly varied. Additionally, 0, 2 and 4cm bump depths are considered at both ends of the bridge. Due to the variability in the point of encounter of both vehicles on the bridge, a vehicle may be leaving the bridge while the other is just entering it, i.e., vehicles meeting very close to the bridge support. Obviously these events do not create critical loading scenarios for bending moment at mid-span but they cause significant shear forces near the supports. For this reason, only the largest 20% of all simulated loading effects are used to obtain Figures 19 and 20.

Figure 19 shows the mean DAF values for Type I meeting events and two bump depths. Note that the shear DAF in this figure refers to the support where the maximum static load effect is generated in each event. Obvious similarities are obtained for Type I meeting events and single vehicle events (Figure 14) although in general DAF values tend to be smaller for the meeting scenarios. In Figure 19a, as in Figure 14a, there is some bump influence in dynamic shear load effects regardless of the span length. On the other hand, bending moment at mid-span (Figure 19b) is influenced by the presence of a expansion joint only in the shortest spans, similarly as for the single vehicle events (Figure 14b).

Figure 19: Mean DAF from Monte Carlo simulations due to Type I meeting events; No damage (•-•-•-•-); 2 cm bump depth (x-x-x-x-), 4 cm bump depth (*-*-*-*-); a) Shear force; b) Mid-span bending moment

Monte Carlo results for Type II events are analysed in terms of DI in Figure 20 and compared to Type I results. DI increments due to damaged expansion joints are generally smaller for meeting events where cranes are involved, for both load effects, shear and bending moment. The highest DI of 0.19 is given by DAF for moment when two 5-axle trucks meet each other driving over 4cm bumps at each end of a 6m span bridge. The same scenario causes the highest DI for shear which is 0.11. For spans equal or greater than 12m, DI hardly varies, and it is less than 0.01 for moment and both meeting events, about 0.05 for shear due to Type I, and less than 0,02 for shear due to Type II.

Figure 20: Shear (dashed line) and bending moment (solid line) dynamic increments due to Type I (•) and Type II (o) meeting events; a) 2cm bump; b) 4cm bump

5 Summary

This paper has shown how the shear load effect is affected by bridge length and a bump prior to the bridge, and how extremely heavy rigid vehicles such as cranes are less sensitive to this irregularity than typical 5 axle articulated trucks. Equation (1) by Eurocode suggests a linear variation of DAF values for both bending and shear load effects from 1.30 (0m span) down to 1.10 (50m span) in two-lane bridges. These values can be more accurately defined if data on the road profile, the bridge length, the condition of the expansion joint and the critical traffic event expected were gathered at the site. For spans longer than 12m, the simulations in this paper have resulted in mean

DAF values that have not exceeded 1.10 regardless of the load effect or traffic event under investigation. For spans shorter than 12m, DAF for shear at the support has been found to be significantly smaller than DAF for mid-span bending. The differences between both DAFs strongly depend on the depth of a bump prior to the bridge and on the governing form of traffic load at the site. The influence of the condition of the expansion joint on DAF has been evaluated through a parameter, DI, that has been related to bridge length. For example, Figure 14 suggests a maximum mean DI of 0.18 for shear and 0.23 for moment in the case of a single 5-axle truck, 5m span and a 4cm bump, but once the bridge length exceeds 20m, the DI remains smaller than 0.06 and 0.02 for shear and bending respectively. However, the governing scenario is more likely to be a single crane crossing or a Type I meeting event, and for those situations DAF and DI values might be further reduced. Based on a road class 'A' with a 2cm bump at the expansion joint, the authors propose the following DAF values for the assessment of two-lane straight bridges: (a) For bending moment, a linear variation from 1.45 in a 5m span to 1.15 in a 12m span, and a constant value of 1.15 for medium spans longer than 12m; (b) For shear, a linear variation from 1.20 in a 5m span to 1.10 in a 24m span, and a constant value of 1.10 for medium span lengths longer than 24m. If there is no sign of a bump at the expansion joint, then DAF can be assumed to vary linearly from 1.25 to 1.15 for spans of 5m and 12m respectively for moment, from 1.15 to 1.10 for shear, and to remain constant as 1.15 and 1.10 for bending and shear respectively in medium spans longer than 12m. These general recommendations can be further tuned using VBI simulations based on experimentally validated models of the particular bridge, traffic loading scenario and profile under investigation.

6 Conclusions

This paper has addressed the need of exploring the dynamics associated to the shear load effect. The influence of shear DAF values has been investigated by comparison of two vehicle configurations, a typical 5-axle truck and a crane truck, as well as meetings of two trucks on a bridge. Using a numerical vehicle-bridge interaction model and Monte Carlo simulation, a sensitivity study has been carried out for many possible bridge spans, speeds, vehicle characteristics, severity of damaged expansion joints and road profiles. A bump prior to the damage has been used to model a damaged expansion joint or discontinuity due to differential settlement. The results clearly show that the highest DAFs for shear occur in shorter spans and that they are directly related to the damage severity of the expansion joint. For meeting events, DAF for shear decreases with bridge spans up to 12m, and then, it remains approximately constant. For a given bump depth and spans shorter than 12m, the mean DAF for shear has been smaller than the mean DAF for bending moment . In the case of spans longer than 12m where two heavy trucks can meet, the DAF for both load effects is more similar, and it has been noticed that the depth of a bump prior to the bridge does not result in significant differences in the mid-span bending moment simulations, while the mean DAF for shear remains to be influenced by the bump size. Furthermore, massive rigid vehicles with a lot of axles like cranes, that could govern the assessment of a bridge, have been shown to be less influenced by large road discontinuities prior to the bridge and tend to produce significantly smaller dynamic increments than 5-axle trucks. Overall, the higher the static load effect is, the lower the dynamic amplification factor for shear forces at supports.

Acknowledgments

The authors would like to express their gratitude for the financial support received from the 6th European Framework Project ARCHES (Assessment and Rehabilitation of Central European Highway Structures) towards this investigation.

References

[1] Brühwiler E, Herwig A. Consideration of dynamic traffic action effects on existing bridges at ultimate limit state. In: Koh, Fragopol, editors. Bridge maintenance, safety, management, health monitoring and informatics. London: Taylor & Francis Group; 2008.

[2] Higgins C, Yim SC, Miller TH, Robelo MJ, Potisuk T. Remaining life of reinforced concrete beams with diagonal-tension cracks. Final report SPR 341, FHWA-OR-RD-04-12, 2004.

[3] Organization for Economic Co-operation and Development. Dynamic interaction between vehicles and infrastructure experiment (DIVINE), 1998. See www.oecd.org/dataoecd/9/22/2754516.pdf for further details.

[4] Competitive and Sustainable Growth Program (GROWTH). Guidance for the Optimal Assessment of Highway Structures (SAMARIS), 2006. See http://samaris.zag.si/documents.htm for further details.

[5] McLean D, Marsh ML. Dynamic impact factors for bridges, National Cooperative Highway Research Program (NCHRP) Synthesis 266, a synthesis

of highway practice., Transportation Research Board, National Research Council (US), 1998.

[6] Kim CW, Kawatani M, Hwang WS. Reduction of traffic-induced vibration of two-girder steel bridge seated on elastomeric bearings. Engineering Structures, 26: 2185-2195, 2004.

[7] Lima JM, Brito J. Inspection survey of 150 expansion joints in road bridges. Engineering Structures, 31(5): 1077-1084, 2009.

[8] Michaltsos GT. Parameters affecting the dynamic response of light (steel) bridges. Facta Universitatis, Series Mechanics, Automatic Control and Robotics, 2(10): 1203-1218, 2000.

[9] Michaltsos GT, Konstantakopoulos TG. Dynamic response of a bridge with surface deck irregularities. Journal of Vibration and Control, 6: 667-689, 2000.

[10] Li Y, OBrien E, González A. The development of a dynamic amplification estimator for bridges with good road profile. Journal of Sound and Vibration, 293(1-2): 125-137, 2006.

[11] Chompooming K, Yener M. The influence of roadway surface irregularities and vehicle deceleration on bridge dynamics using the method of lines. Journal of Sound and Vibration, 183(4): 567–589, 1995.

[12] Moghimi H, Ronagh HR. Development of a numerical model for bridge-vehicle interaction and human response to traffic-induced vibration. Engineering Structures, 30: 3808-3819, 2008.

[13] Frýba L. Vibration of solids and structures under moving loads. Groningen: Noordhoff, 1999.

[14] Yang YB, Yau JD, Wu YS. Vehicle-bridge interaction dynamics. Singapore: World Scientific, 2004.

[15] Savin E. Dynamic amplification factor and response spectrum for the evaluation of vibrations of beams under successive moving loads. Journal of Sound and Vibration, 248(2): 267-288, 2001.

[16] Pesterev AV, Bergman LA, Tan CA, Tsao TC, Yang B. On asymptotics of the solution of the moving oscillator problem. Journal of Sound and Vibration, 260: 519-536, 2003.

[17] Cojocaru EC, Irschik H, Gattringer H. Dynamic response of an elastic bridge due to moving elastic beam. Computers & Structures 82: 931-943, 2004.

[18] Huang D, Wang TL, Shahawy M. Vibration of horizontally curved box girder bridges due to vehicles. Computers & Structures, 68: 513-528, 1998.

[19] Huang D. Dynamic loading of curved steel box girder bridges due to moving vehicles. Structural Engineering International, 4: 365-372, 2008.

[20] Wu YS, Yang YB. Steady-state response and riding comfort of trains moving over a series of simply supported bridges. Engineering Structures, 25: 251-265, 2003.

[21] American Association of State Highway and Transportation Officials. AASHTO Standard specifications for Highway bridges, 16th Ed., Washington D.C., USA, 1996.

[22] American Association of State Highway and Transportation Officials. AASHTO LRFD Bridge Design Specifications, 5th Ed., Washington D.C., USA, 2010.

[23] British Standards institution. Eurocode 1: Actions on structures – Part 2: Traffic loads on bridges (BS EN 1991-2), BSI, 2003.

[24] Dawe P. Research perspectives: Traffic loading on highway bridges. London: Thomas Telford, 2003.

[25] OBrien E, Enright B, Caprani C. Implications of future heavier trucks for Europe's bridges. In: Transport research arena Europe, Ljubljana, 2008.

[26] González A, Cantero D, OBrien E.J.The impact of a bump on the response of a bridge to traffic. In: B.H.V. Topping, L.F. Costa Neves, R.C. Barros, editors. Proceedings of the twelfth international conference on civil, structural and environmental engineering computing. Stirlingshire, UK: Civil-Comp press; 2009.

[27] Weaver W, Johnston PR. Structural dynamics by finite elements. Prentice-Hall, 1987.

[28] Cantero D, OBrien EJ, González A. Modelling the vehicle in vehicle-infrastructure dynamic interaction studies. Proceedings of the institution of Mechanical Engineers, Part K, Journal of Multi-body dynamics, 224(2): 243-248, 2010.

[29] Wang TL, Huang D. Computer modelling analysis in bridge evaluation. Florida: International University, Miami, 1992.

[30] Gillespie TD, McAdam CC, Hu GT, Bernard JE, Winkler CB. Simulation of effects of increased truck size and weight. Michigan: Ann Arbor, 1979.

[31] Cebon D. Interaction between heavy vehicles and roads. Society of automotive engineers, SP-951, 1993.

[32] Harris NK, OBrien EJ, González A. Reduction of bridge dynamic amplification through adjustment of vehicle suspension damping. Journal of Sound and Vibration, 302(3): 471-485, 2001.

[33] Cantero D, González A, OBrien EJ. Maximum dynamic stress on bridges traversed by moving loads. Proceedings of the Institution of Civil Engineers, Bridge Engineering, 162(2): 75-85, 2009.

[34] Li H. Dynamic response of highway bridges to heavy vehicles, Ph.D. Thesis, Florida state university, 2005. For further information see: http://etd.lib.fsu.edu.

[35] Lehtonen T, Kaijalainen O, Pirjola H, Juhala M. Measuring stiffness and damping properties of heavy vehicles. Society of automotive engineers of Japan (FISITA), 1-11, 2006.

[36] Fu TT, Cebon D. Analysis of truck suspension database. International journal of heavy vehicle systems 9(4): 281-297, 2002.

[37] Kirkegaard PH, Nielsen SRK, Enevoldsen I. Heavy vehicles on minor highway bridges – Dynamic modelling of vehicles and bridges. Department of Building Technology and Structural Engineering, Aalborg University, 1997.

[38] Wong JY. Theory of ground vehicles. John Wiley & sons, 1993.

[39] Dominguez J. Dinamica de puentes de ferrocarril para alta velocidad: metodos de calculo y estudio de la resonancia, Ph.D. Thesis, Department of continuum mechanics, Polytechnic University of Madrid, 2001. Further information see: http://oa.upm.es/1311/

[40] OBrien EJ, Keogh D. Bridge deck analysis. E & FN Spon, 1999.

[41] Esmailzadeh E, Ghorashi M. Vibration analysis of a Timoshenko beam subject to a travelling mass. Journal of Sound and Vibration, 199(4): 615-628, 1997.

[42] Seetapan P, Chucheepsakul S. Dynamic response of a two-span beam subjected to high speed 2DOF sprung vehicles. International Journal of Structural Stability and Dynamics, 6(3): 413-430, 2006.

[43] Hanchi K, Fafard M, Dhatt G, Talbot M. Dynamic behaviour of multi-span beams under moving loads. Journal of Sound and Vibration, 199(1):33-50, 1997.

[44] Sakib MS. Hastening convergence of the orthotropic plate solutions of bridge deck analysis, Master Thesis, Department of Civil Engineering, University of Toronto, 2000. For further information see: https://tspace.library.utoronto.ca/handle/1807/15187

[45] Li Y. Factors affecting the dynamic interaction of bridges and vehicle loads, Ph.D. Thesis, Department of Civil Engineering, University College Dublin, 2006.

[46] Memory TJ, Thambiratnam DP, Brameld GH. Free vibration analysis of bridges. Engineering Structures, 17(10): 705-713, 1995.

[47] International organization for standardization. Mechanical vibration-road surface profiles - Reporting of measure data (ISO 8608), 1995.

[48] Kim CW, Kawatani M. Probabilistic investigation on dynamic response of deck slabs of highway bridges. System Modelling and Optimization, 166: 217-228, 2005.

[49] Kim CW, Kawatani M, Kwon YR. Impact coefficient of reinforced concrete slab on a steel girder bridge. Engineering Structures, 29: 576-590, 2007.

[50] González A, OBrien EJ, Cantero D, Yingyan L, Dowling J, Žnidarič A. Critical speed for the dynamics of truck events on bridges with a smooth surface. Journal of Sound and Vibration, 329(11): 2127-2146, 2010.

[51] González A, Rattigan P, OBrien EJ, Caprani C. Determination of bridge lifetime DAF using finite element analysis of critical loading scenarios. Engineering Structures, 30(9): 2330-2337, 2008.

Figure captions

Figure 1: Dynamic amplification factors for failure modes with small deformation [1]

Figure 2: Vehicle model sketch; a) 5-axle truck; b) Crane (all dimensions in m)

Figure 3: Bridge model

Figure 4: a) Damaged expansion joint (all dimensions in cm, *h*: bump height); b) Example of road profile with 2cm deep bump

Figure 5: Dynamic amplification factors versus frequency ratio due to a moving constant load; shear at 1st support (solid line), bending moment (dotted line), shear at 2nd support (dashed line)

Figure 6: Dynamic amplification factors versus speed due to a constant load moving on a 12m bridge for; a) bending moment; b) shear at 2nd support

Figure 7: Mid-span bending moment response of a 12m bridge due to a single constant load travelling at speed of 56km/h; total bending moment (solid line), static component (dashed line), dynamic contribution of inertial forces due to 1st mode (dotted line)

Figure 8: Shear response at 2nd support of a 12m bridge due to a single constant load travelling at a speed of 82km/h; total shear force (solid line), static component (dashed line), dynamic contribution of inertial forces due to 1st mode (dotted line)

Figure 9: Dynamic contribution of inertial forces of the bridge to the shear at 2nd support of a 12m bridge due to a single constant load travelling at a speed of 82km/h; 1st mode (solid line), 2nd mode (dashed line), 3rd mode (dotted line)

Figure 10: Dynamic amplification factors versus speed for a 5-axle truck model consisting of constant loads on a 12 m bridge; shear at 1st support (solid line), bending moment (dotted line), shear at 2nd support (dashed line)

Figure 11: Total (solid line), static (dashed line) and inertial (dotted line) components for load effects due to a 5-axle truck travelling at 60km/h on a 12m span with a 2cm bump; a) Mid-span bending moment; b) Shear force at 1st support

Figure 12: Shear 1st support (solid line), Shear 2nd support (dashed line) and bending moment mid-span (dotted line) due to a 5-axle truck on a 12m span with a smooth profile; a) Dynamic amplification factors without a bump; b) Dynamic increments due to a 2cm bump

Figure 13: Shear 1st support (solid line), shear 2nd support (dashed line) and bending moment mid-span (dotted line) due to a 5-axle truck on 12m span with a class 'A' road profile; a) Dynamic amplification factors (mean value) without a bump; b) Dynamic amplification factors (standard deviation) without a bump; c) Mean dynamic increments due to a 2cm bump

Figure 14: Mean DAF due to fleet of 5-axle trucks on class 'A' profile; No damage (•-•-•-•-); 2cm bump depth (x-x-x-x-), 4cm bump depth (*-*-*-*-); a) Shear force at 1st support; b) Bending moment; c) Shear force at 2nd support

Figure 15: Standard deviation of DAF due to fleet of 5-axle trucks on class 'A' profile; No damage (•-•-•-•-); 2cm bump depth (x-x-x-x-), 4cm bump depth (*-*-*-*-); a) Shear force at 1st support; b) Bending moment; c) Shear force at 2nd support

Figure 16: Mean DAF due to fleet of cranes on class 'A' profile; No damage (•-•-•-•-); 2cm bump depth (x-x-x-x-), 4cm bump depth (*-*-*-*-); a) Shear force at 1st support; b) Bending moment; c) Shear force at 2nd support

Figure 17: Standard deviation of DAF due to fleet of cranes on class 'A' profile; No damage (•-•-•-•-); 2cm bump depth (x-x-x-x-), 4cm bump depth (*-*-*-*-); a) Shear force at 1st support; b) Bending moment; c) Shear force at 2nd support

Figure 18: Scenarios of vehicle meeting events; a) Type I; b) Type II

Figure 19: Mean DAF from Monte Carlo simulations due to Type I meeting events; No damage (•-•-•-•-); 2 cm bump depth (x-x-x-x-), 4 cm bump depth (*-*-*-*-); a) Shear Force; b) Mid-span bending moment

Figure 20: Shear (dashed line) and bending moment (solid line) dynamic increments due to Type I (•) and Type II (o) meeting events; a) 2cm bump; b) 4cm bump

Table captions

Table 1: Truck and crane mechanical parameters

Table 2: General characteristics of the bridge models

Table 3: Mean and standard deviation of shear force at 1st support due to single vehicle events

Figure 1: Dynamic amplification factors for failure modes with small deformation [1]

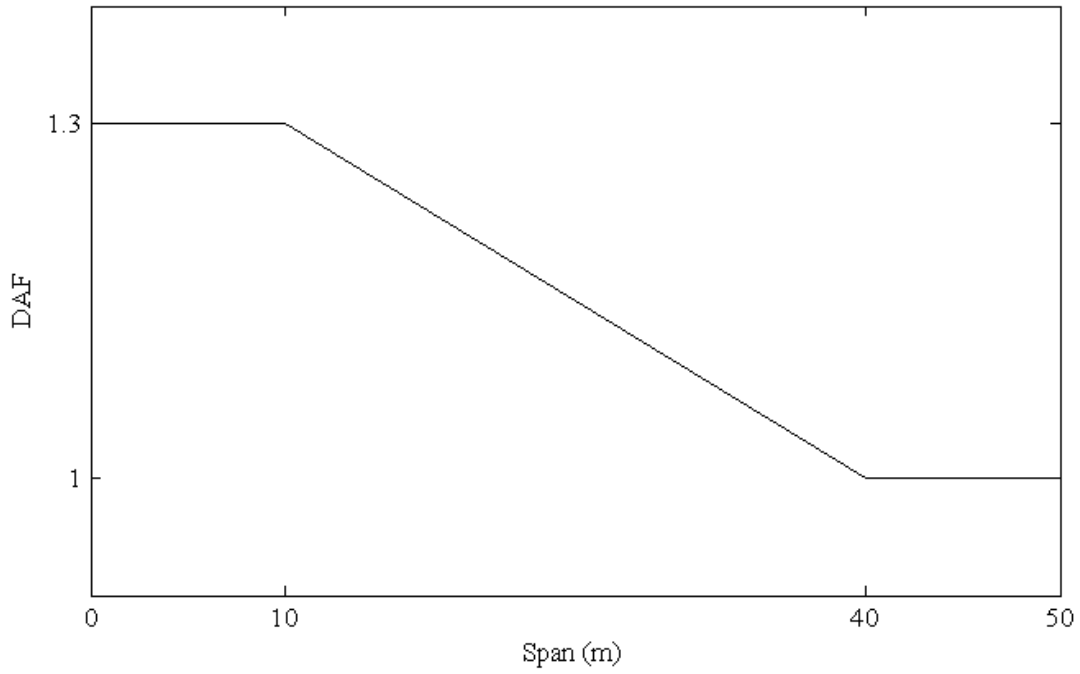

Figure 2: Vehicle model sketch; a) 5-axle truck; b) Crane (all dimensions in m)

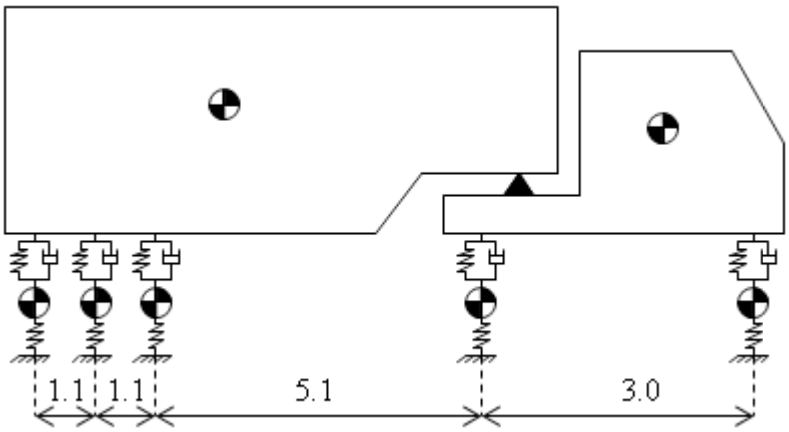

(a)

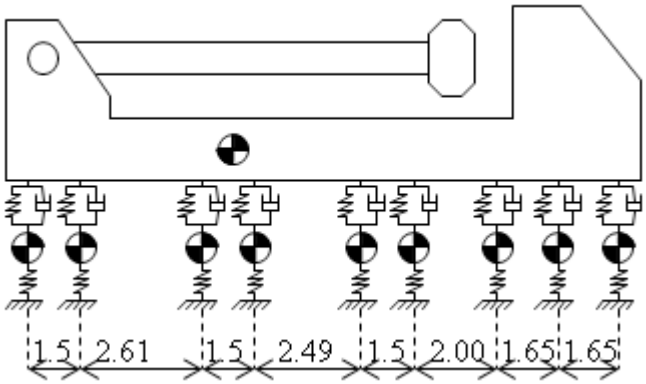

(b)

Figure 3: Bridge model

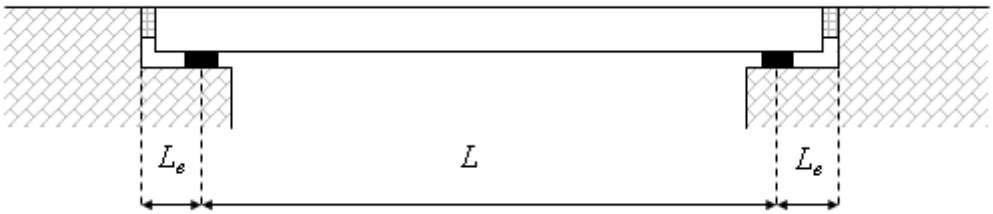

Figure 4: a) Damaged expansion joint (all dimensions in cm, *h*: bump height); b) Example of road profile with 2cm deep bump

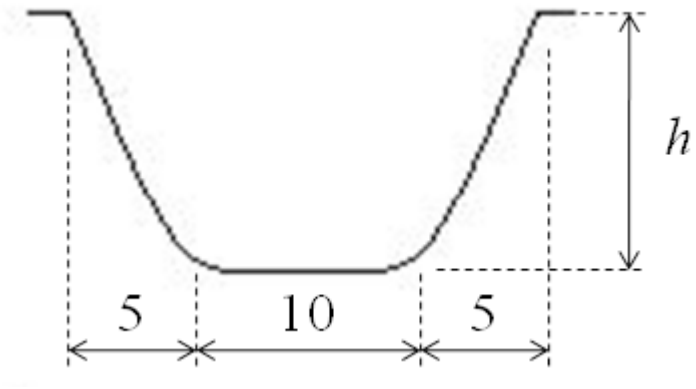

(a)

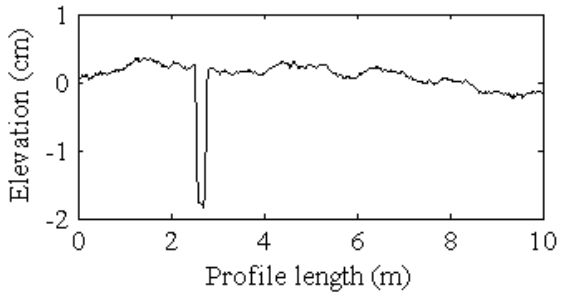

(b)

Figure 5: Dynamic amplification factors versus frequency ratio due to a moving constant load; shear at 1st support (solid line), bending moment (dotted line), shear at 2nd support (dashed line)

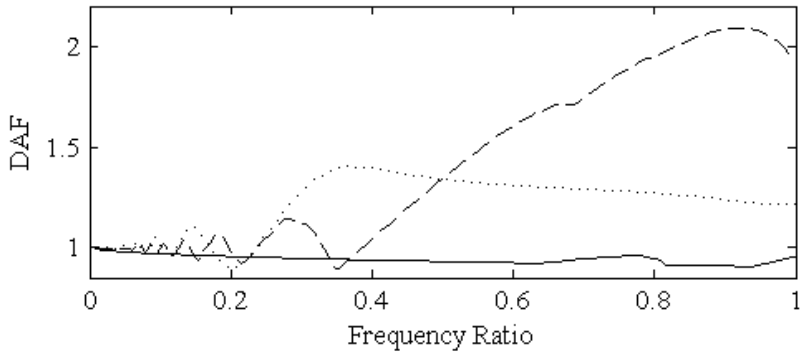

Figure 6: Dynamic amplification factors versus speed due to a constant load moving on a 12m bridge for; a) bending moment; b) shear at 2nd support

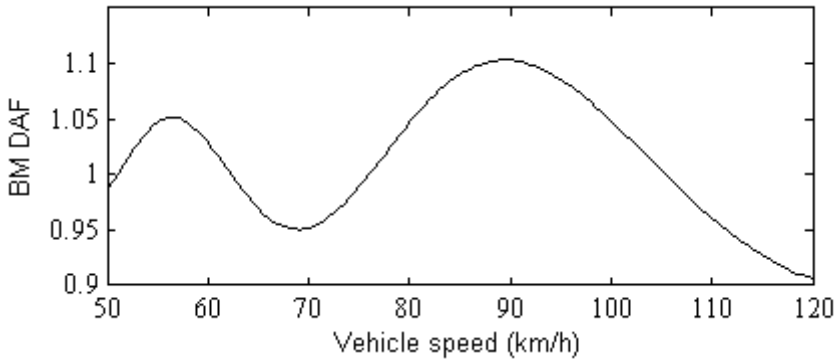

(a)

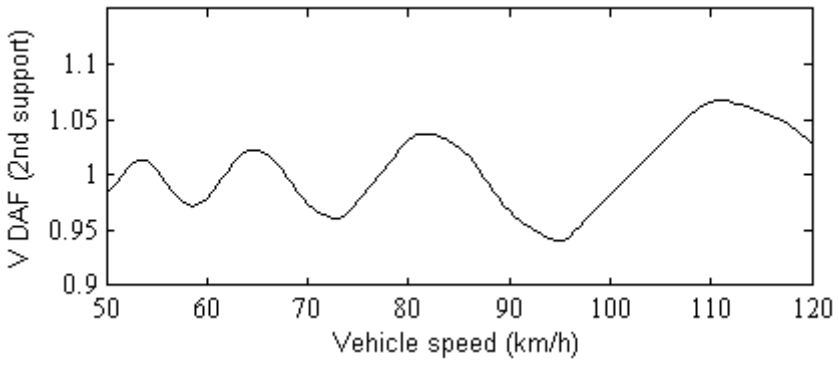

(b)

Figure 7: Mid-span bending moment response of a 12m bridge due to a single constant load travelling at speed of 56km/h; total bending moment (solid line), static component (dashed line), dynamic contribution of inertial forces due to 1st mode (dotted line)

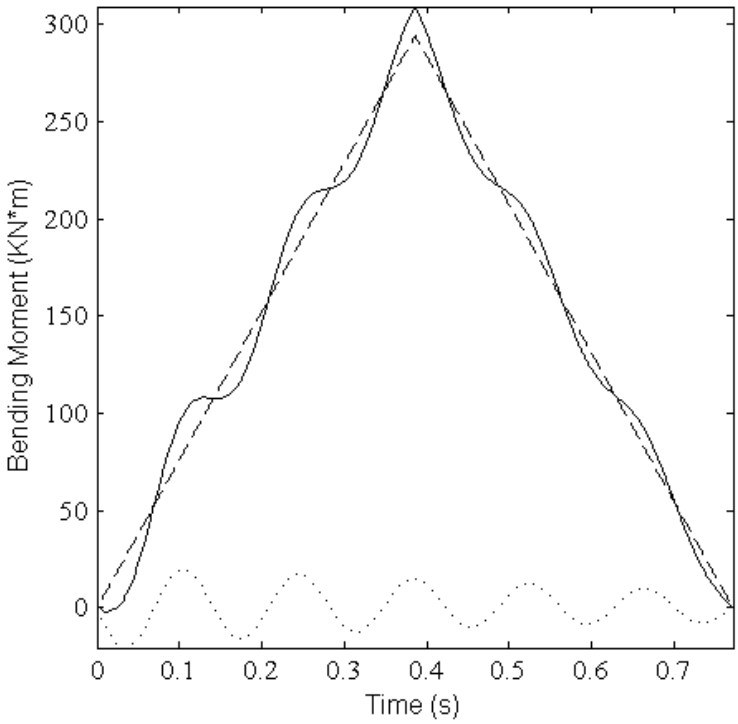

Figure 8: Shear response at 2nd support of a 12m bridge due to a single constant load travelling at a speed of 82km/h; total shear force (solid line), static component (dashed line), dynamic contribution of inertial forces due to 1st mode (dotted line)

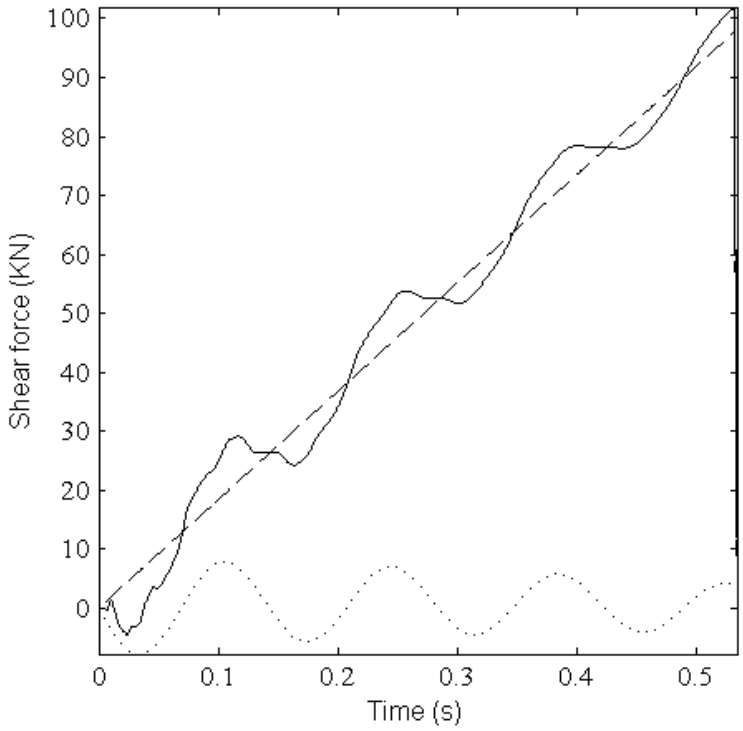

Figure 9: Dynamic contribution of inertial forces of the bridge to the shear at 2nd support of a 12m bridge due to a single constant load travelling at a speed of 82km/h; 1st mode (solid line), 2nd mode (dashed line), 3rd mode (dotted line)

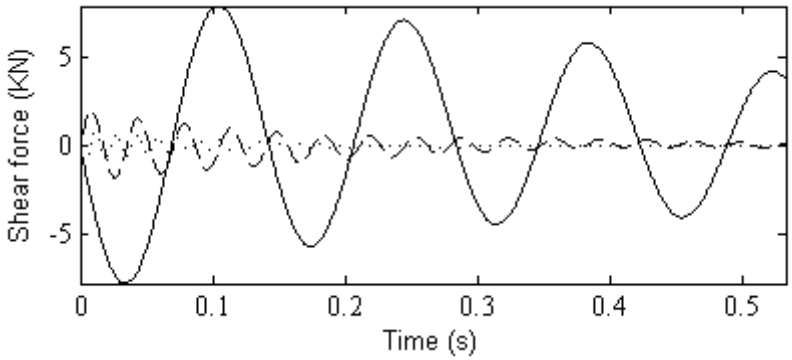

Figure 10: Dynamic amplification factors versus speed for a 5-axle truck model consisting of constant loads on a 12 m bridge; shear at 1st support (solid line), bending moment (dotted line), shear at 2nd support (dashed line)

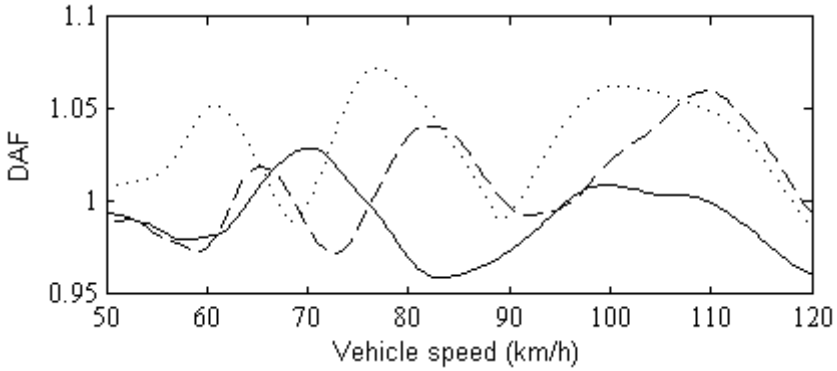

Figure 11: Total (solid line), static (dashed line) and inertial (dotted line) components for load effects due to a 5-axle truck travelling at 60km/h on a 12m span with a 2cm bump; a) Mid-span bending moment; b) Shear force at 1st support

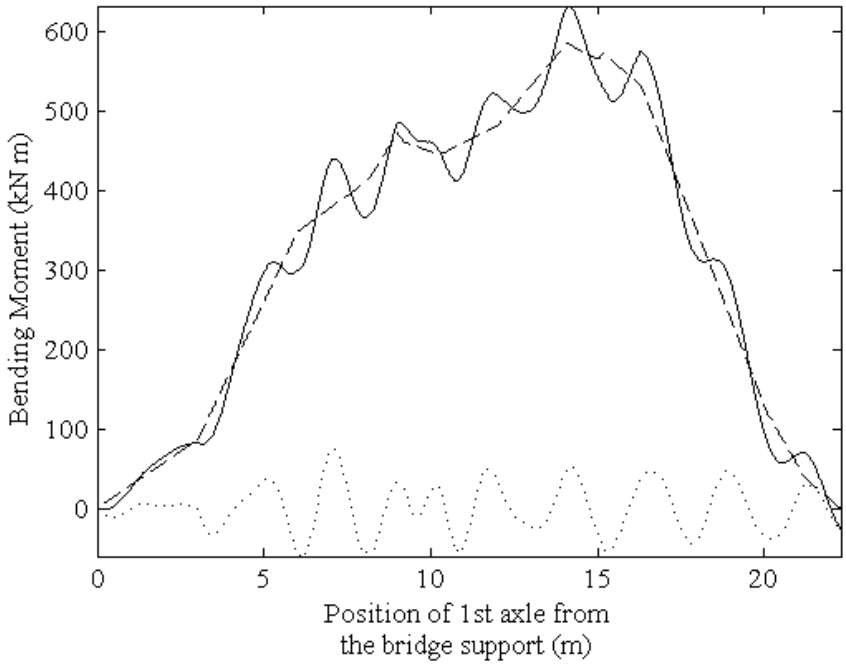

(a)

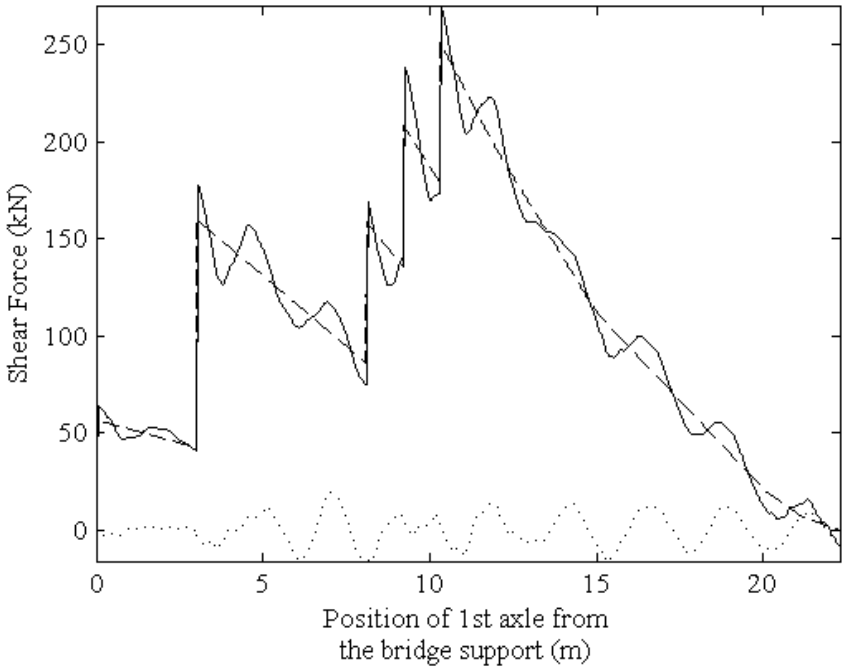

(b)

Figure 12: Shear 1st support (solid line), Shear 2nd support (dashed line) and bending moment mid-span (dotted line) due to a 5-axle truck on a 12m span with a smooth profile; a) Dynamic amplification factors without a bump; b) Dynamic increments due to a 2cm bump

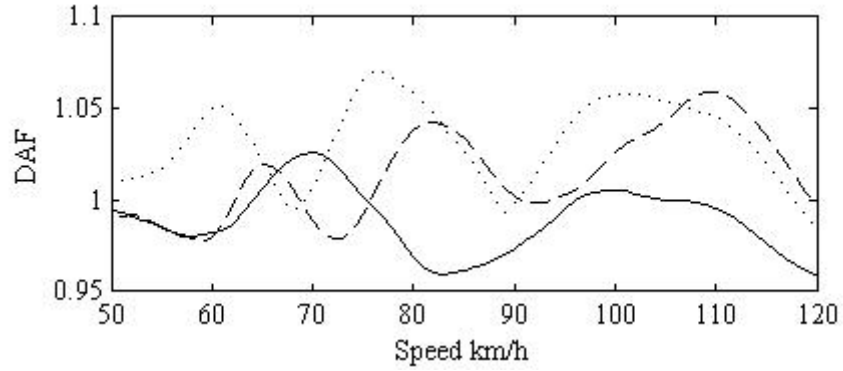

(a)

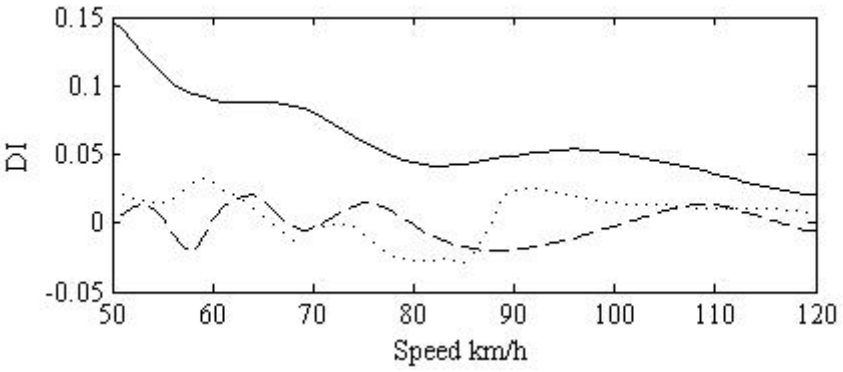

(b)

Figure 13: Shear 1st support (solid line), shear 2nd support (dashed line) and bending moment mid-span (dotted line) due to a 5-axle truck on 12m span with a class 'A' road profile; a) Dynamic amplification factors (mean value) without a bump; b) Dynamic amplification factors (standard deviation) without a bump; c) Mean dynamic increments due to a 2cm bump

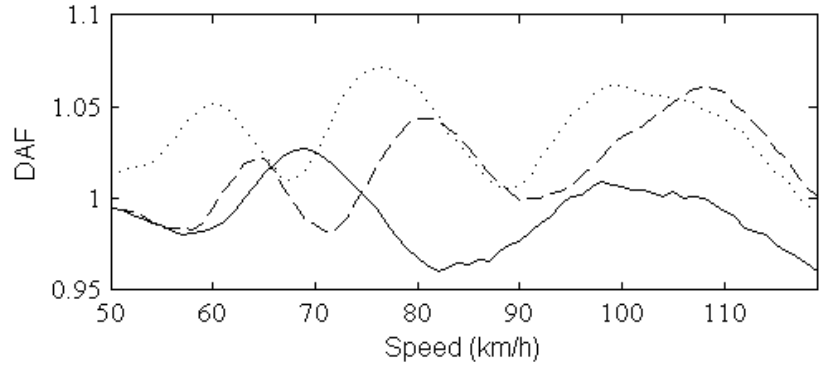

(a)

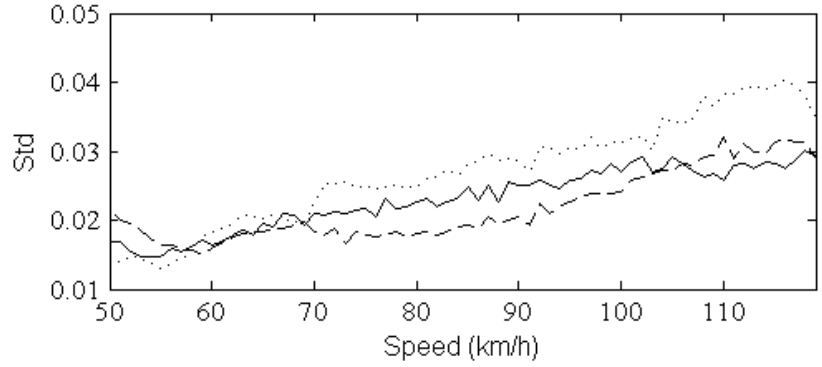

(b)

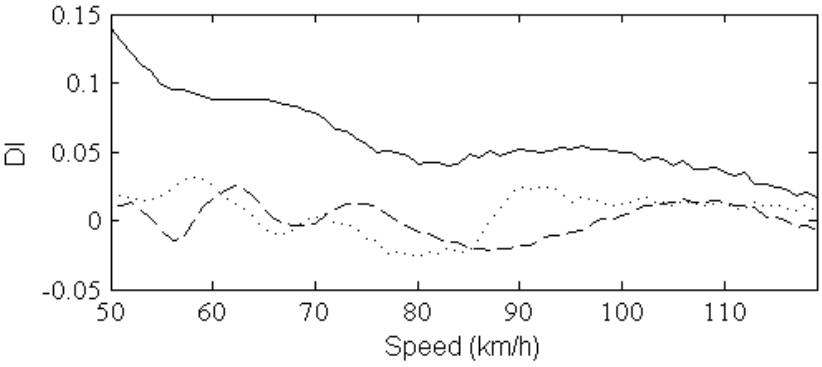

(c)

Figure 14: Mean DAF due to fleet of 5-axle trucks on class 'A' profile; No damage (•-•-•-•-); 2cm bump depth (x-x-x-x-), 4cm bump depth (*-*-*-*-); a) Shear force at 1st support; b) Bending moment; c) Shear force at 2nd support

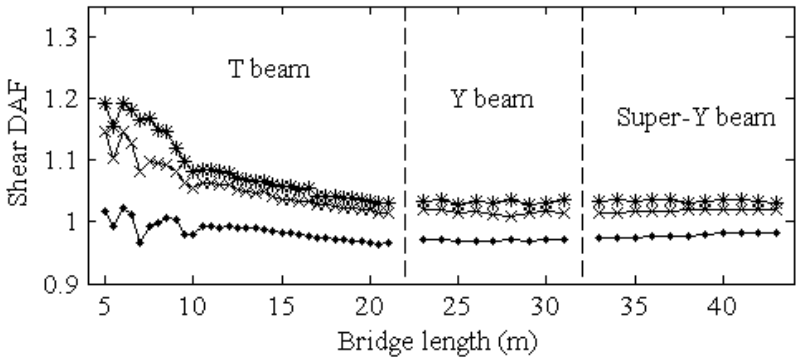

(a)

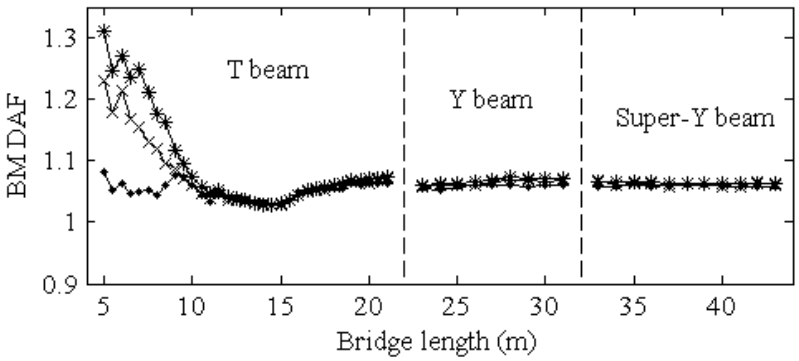

(b)

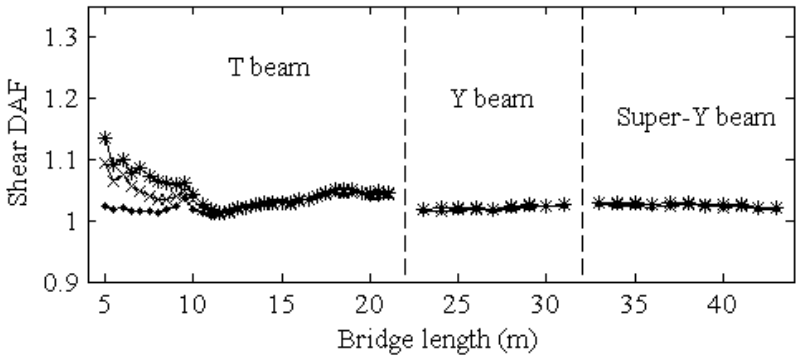

(c)

Figure 15: Standard deviation of DAF due to fleet of 5-axle trucks on class 'A' profile; No damage (•-•-•-•-); 2cm bump depth (x-x-x-x-), 4cm bump depth (*-*-*-*-); a) Shear force at 1st support; b) Bending moment; c) Shear force at 2nd support

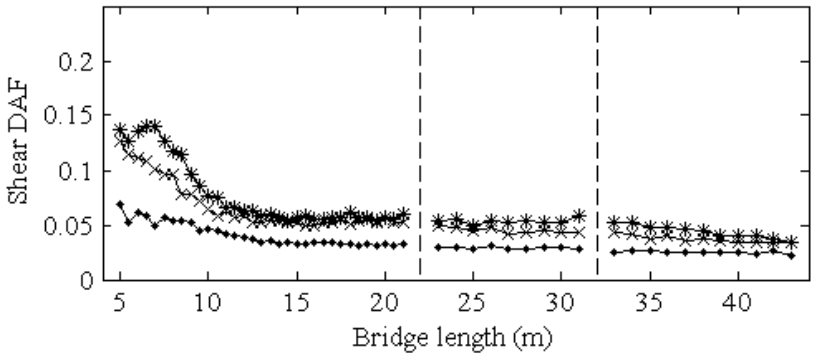

(a)

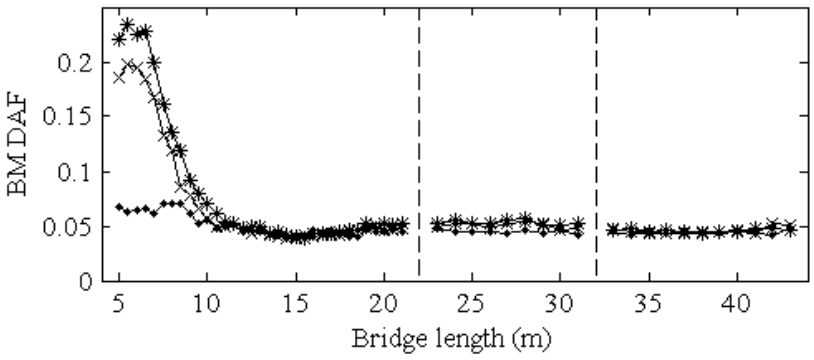

(b)

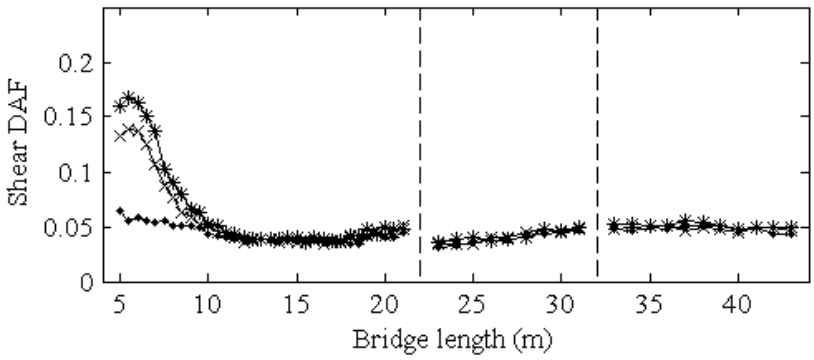

(c)

Figure 16: Mean DAF due to fleet of cranes on class 'A' profile; No damage (•-•-•-•-); 2cm bump depth (x-x-x-x-), 4cm bump depth (*-*-*-*-); a) Shear force at 1st support; b) Bending moment; c) Shear force at 2nd support

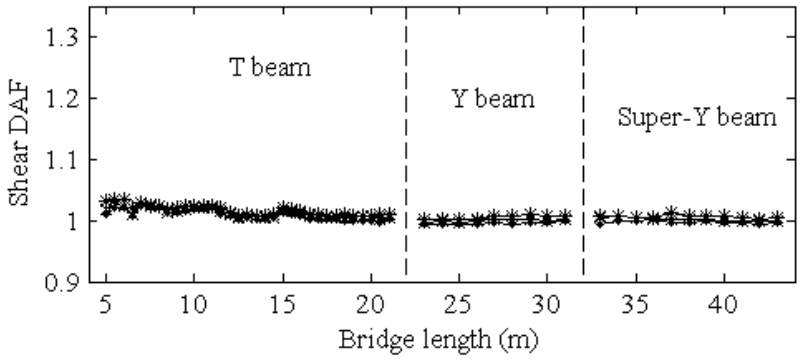

(a)

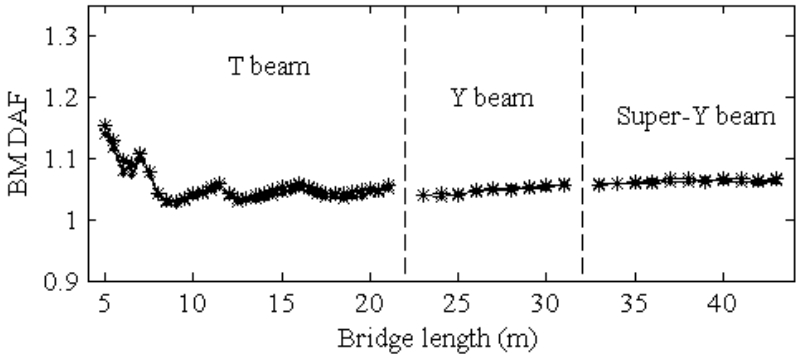

(b)

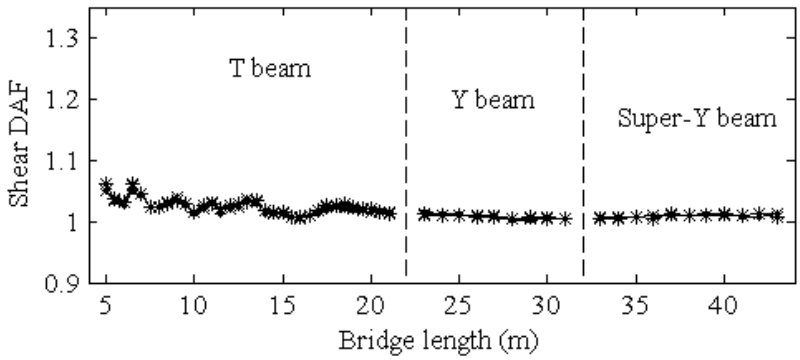

(c)

Figure 17: Standard deviation of DAF due to fleet of cranes on class 'A' profile; No damage (•-•-•-•-); 2cm bump depth (x-x-x-x-), 4cm bump depth (*-*-*-*-); a) Shear force at 1st support; b) Bending moment; c) Shear force at 2nd support

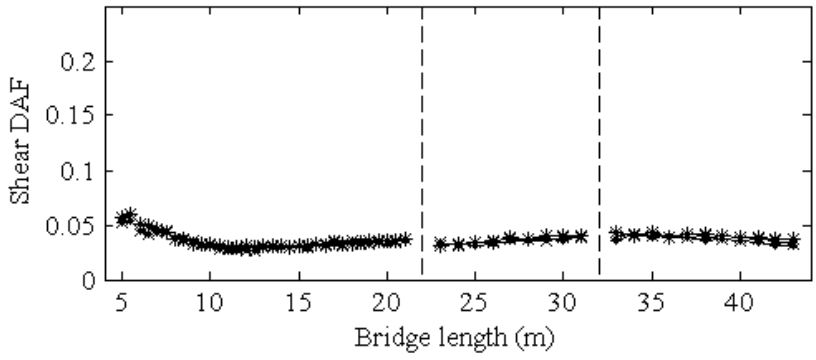

(a)

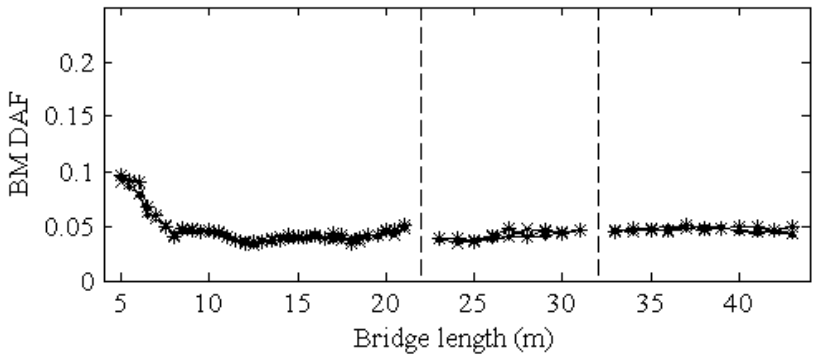

(b)

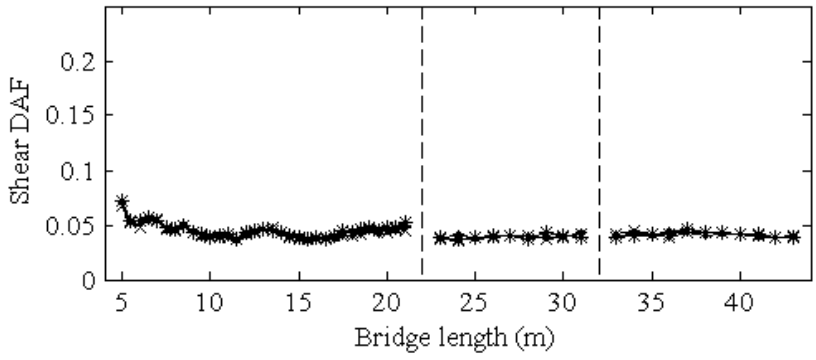

(c)

Figure 18: Scenarios of vehicle meeting events; a) Type I; b) Type II

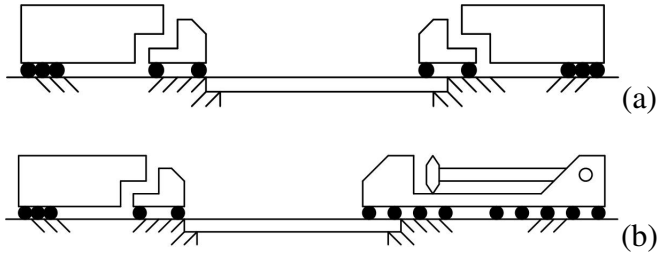

Figure 19: Mean DAF from Monte Carlo simulations due to Type I meeting events; No damage (•-•-•-•-); 2 cm bump depth (x-x-x-x-), 4 cm bump depth (*-*-*-*-); a) Shear Force; b) Mid-span bending moment

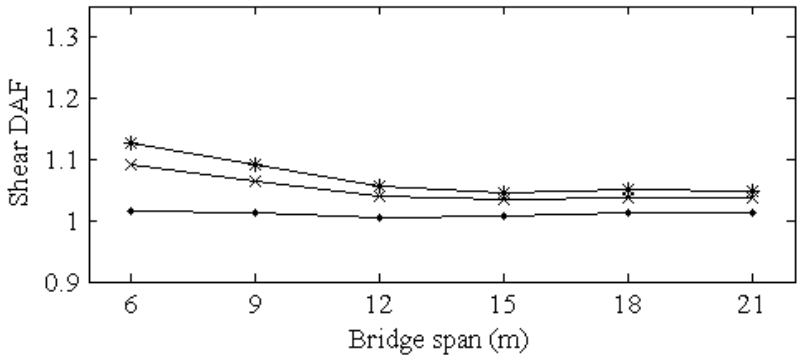

(a)

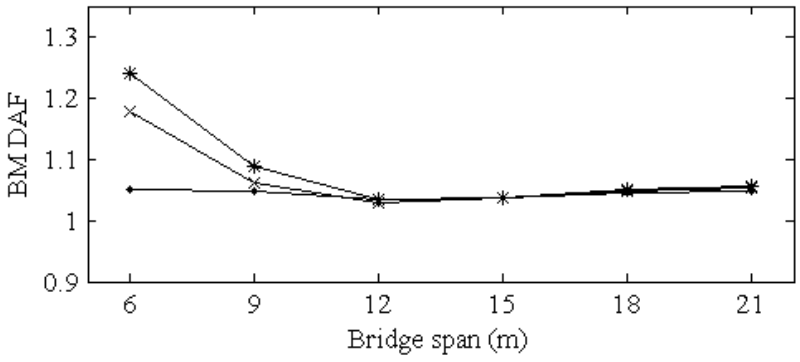

(b)

Figure 20: Shear (dashed line) and bending moment (solid line) dynamic increments due to Type I (•) and Type II (o) meeting events; a) 2cm bump; b) 4cm bump

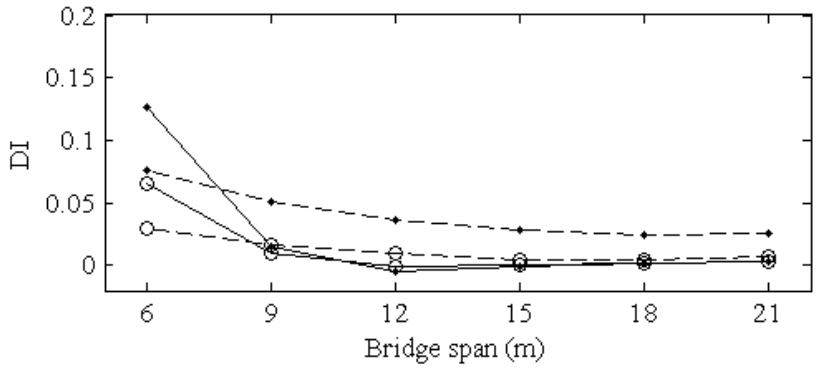

(a)

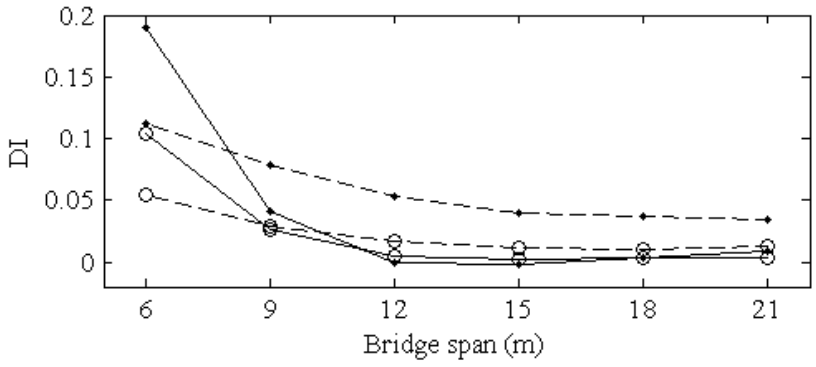

(b)

Table 1: Truck and crane mechanical parameters

5-axle truck		Mean	Std. Dev.	Min.	Max.	Ref.
Masses (kg)	Tractor	4500	-	-	-	[32,
	Semitrailer	31450	-	-	-	36,
	Tractor front axle	700	100	500	1000	37]
	Tractor rear axle	1000	150	700	1300	
	Semitrailer axles	800	100	600	1000	
Suspension stiffness (kN/m)	Tractor, front (air)	600	140	300	1000	[36]
	Tractor, rear (steel)	1000	100	600	1200	
	Tractor, rear (steel)	2000	600	1200	3000	
	Semitrailer (air)	800	200	500	1200	
	Semitrailer (steel)	2500	400	2000	3000	
Suspension damping (kNs/m)		10	2	3	10	[37]
Tyre stiffness (kN/m)	Tractor, front	1500	400	1000	3000	[32,
	Tractor, rear & semitrailer	3000	800	2000	6000	38]
Crane						
Masses (kg)	Body	101700	-	-	-	[37]
	Axles	700	300	500	1000	
Suspension stiffness (kN/m)		8000	80000	3000	160000	[34]
Suspension damping (kNs/m)		40	15	30	60	[34]
Tyre stiffness (kN/m)		2000	1000	1400	3600	[35,38]

Table 2: General characteristics of the bridge models

Type	Length (m)	Mass per unit length (kg/m)	Second moment of inertia (m^4)	1st natural frequency (Hz)
T beams	6	13875	0.0479	15.16
	9	16875	0.1139	9.43
	12	22500	0.2757	7.14
	15	28125	0.5273	5.66
	18	33750	0.9197	4.73
	21	39375	1.4470	4.04
Y beams	23	17419	1.1133	4.44
	27	19372	1.7055	3.78
	31	21650	2.4651	3.26
Super-Y beams	33	20952	2.9327	3.19
	37	22552	3.9425	2.84
	43	24952	5.7957	2.42

Table 3: Mean and standard deviation of shear force at 1st support due to single vehicle events

		5-axle			Crane		
		Bump depth (cm)			Bump depth (cm)		
Span (m)		0	2	4	0	2	4
5	Mean	171.78	193.79	201.7	238.5	239.25	242.81
	St. Dev.	11.70	21.40	23.33	12.35	12.21	13.35
7.5	Mean	185.81	208.59	217.89	327.95	331.27	331.2
	St. Dev.	10.75	18.24	23.75	14.00	14.36	13.88
10	Mean	221.25	237.34	241.96	394.38	396.68	397.54
	St.Dev.	10.44	14.48	17.25	12.13	12.05	12.42
12.5	Mean	253.88	271.44	275.35	461.98	462.31	463.76
	St.Dev.	9.39	13.62	16.34	12.57	12.46	13.93
15	Mean	274.15	290.79	295.4	529.12	527.77	533.09
	St.Dev.	9.27	14.76	16.02	16.03	15.82	16.50